The mutant isocitrate dehydrogenase 1 product, 2-hydroxyglutarate, activates MutT homolog 1 in glioma cells via the augmentation of reactive oxygen species levels

BHARATHAN BHAVYA[1*], CHELLAPAN REGHUVARAN ANAND[1*], MADHUSOODANAN URULANGODI[1], KALAPURAKKAL SREELAKSHMI[1], AKKIHEBBAL NARASIMHAIAH DEEPTI[2], GIRISH RAMACHANDRAN MENON[3,4], KRISHNAKUMAR KESAVAPISHARADY[3], HARIHARAN VENKAT EASWER[3] and SRINIVAS GOPALA[1]

Departments of [1]Biochemistry, [2]Pathology and [3]Neurosurgery, Sree Chitra Tirunal Institute for Medical Sciences and Technology, Thiruvananthapuram, Kerala 695011, India

Received June 5, 2022; Accepted September 30, 2022

DOI: 10.3892/wasj.2022.174

Abstract. MutT homolog1 (MTH1) is an enzyme responsible for removing oxidized nucleotides from cells. The activation of MTH1 has been reported in a number of cancer cell types and is considered to be responsible for imparting resistance towards anticancer drugs. While there are several known mechanisms for the activation of MTH1 in cancer cells, the present study aimed to evaluate the role of mutant isocitrate dehydrogenase1 (mIDH1)-mediated reactive oxygen species (ROS) production in the activation of MTH1 in glioma cells. MTH1 was found to be upregulated in both mIDH1-expressing cells and 2-hydroxyglutarate (2-HG)-treated cells. mIDH1 and its product, 2-HG, increased the levels of ROS in cultured glioblastoma cells. Furthermore, the increased expression and activity of MTH1 were observed in glioma tissues harboring mIDH1 compared to tissues with wild-type IDH1. On the whole, the findings of the present study unveil a novel mechanism of activation of MTH1 in glioma cells harboring mutant IDH1.

Correspondence to: Dr Srinivas Gopala, Department of Biochemistry, Sree Chitra Tirunal Institute for Medical Sciences and Technology, Medical College PO, Thiruvananthapuram, Kerala 695011, India
E-mail: srinivasg@sctimst.ac.in

Present address: [4]Department of Neurosurgery, Kasturba Hospital, Manipal, Karnataka 576104, India

[*]Contributed equally

Abbreviations: MTH1, MutT homolog 1; ROS, reactive oxygen species; mIDH1, mutant isocitrate dehydrogenase 1; wt-IDH1, wild type-isocitrate dehydrogenase 1; 2-HG, 2-hydroxyglutarate; 8-oxodG, 8-oxo-7,8-dihydro-2'-deoxyguanosine

Key words: MTH1, mIDH1, glioma, tumorigenesis, reactive oxygen species

Introduction

Isocitrate dehydrogenase (IDH) enzymes are key players in various metabolic processes, such as the tricarboxylic acid cycle, lipogenesis, glutamine metabolism and redox regulation (1). These $NAD(P)^+$-dependent enzymes catalyze the conversion of isocitrate to α-ketoglutarate (α-KG) via oxidative decarboxylation and generates NAD(P)H (2). Mutations in IDH1 were first identified in human glioma tissue biopsies by whole genome sequencing, and it was observed that the mutations occur in a large fraction of patients with secondary glioblastoma (3). The most critical is a point mutation where arginine is replaced by histidine (R132H) at the 132nd position. The IDH1 mutation status is currently included as an essential criterion for glioma classification by the World Health Organization classification of the Central Nervous System Tumors (4,5).

It has been previously reported that IDH1 mutation generates increased levels of reactive oxygen species (ROS) in cells via its enzymatic product, 2-hydroxyglutarate (2-HG) (6). The generated ROS can thus interact with several biomolecules, leading to the activation of signaling events and consequently to robust responses, such as the activation of the antioxidant pathway and DNA damage repair pathways. Among these, the ROS-mediated activation of various sanitation enzymes, such as MutT homolog1 (MTH1) has been reported (7). MTH1 belongs to a superfamily of enzymes known as the nucleoside diphosphates linked to moiety-X (NUDIX) hydrolases and is potentially the only enzyme involved in preventing mutations in DNA (8). In a previous study, the authors reported that the silencing of MTH1 affected glioma cell migration and invasion, and inhibited the regulators of angiogenesis (9).

In the present study, it was hypothesized that mutant IDH1 (mIDH1) and its product, 2-HG, is responsible for the activation of MTH1, via the production of ROS. To examine this hypothesis, two human cell lines [U87 (glioblastoma of unknown origin) and U251 (astrocytoma)] were transfected with mIDH1 plasmid and MTH1 expression was examined in these cells. The mIDH1-expressing cells exhibited an

increased MTH1 expression. When 2-HG, a product of mIDH1 enzyme, was exogenously supplied to the cells, MTH1 expression was found to be significantly elevated. The results also suggested that 2-HG was a major contributor of increased ROS generation in mIDH1-expressing cells. In order to verify the aforementioned findings obtained using the cell lines, MTH1 expression levels/activity was examined in IDH1 wild-type (wt) gliomas and gliomas with IDH1 mutation. A positive correlation was also found between MTH1 and mIDH1 expression in glioma patient biopsies. Consistent with this finding, the 8-oxo-7,8-dihydro-2'-deoxyguanosine (8-oxo-dG) levels, which are indicative of MTH1 activity, were found to be higher in the mIDH1-harboring glioma biopsies than the wt-IDH1 biopsies. On the whole, the present study provides evidence of the role of mIDH1/2-HG-mediated ROS production in the activation of MTH1 in both mIDH1 glioma cell lines and in glioma tissues harboring mIDH1.

Materials and methods

Collection of tissue biopsies. Human glioma tissue biopsies were collected (from January, 2017 to December, 2019) from the Department of Neurosurgery, Sree Chitra Tirunal Institute for Medical Sciences and Technology, Trivandrum, India, according to the protocols approved by the Institutional Ethical Committee (Institutional Ethics Committee Approval no. SCT/IEC/932/AUGUST-2016). In total, 57 glioma biopsies were selected for the study (30 samples with wild-type IDH1 and 27 samples carrying the IDH mutation). The patients selected for the study were in the age range of 7-65 years with a median age of 42. Informed written consent was obtained from the patients or relatives prior to tissue collection and processing, which has been previously described (9). For patients who were <18 years of age, consent was obtained by the parents of those patients. A summary of patient characteristics is presented in Table I.

Cell culture, plasmid DNA isolation and transfection. The U87MG cells (glioblastoma of unknown origin) and the U251MG human astrocytoma cell line used in the experiments were procured from the National Centre for Cell Science (NCCS, Pune, India). The U87MG cells were authenticated at NCCS using short tandem repeat (STR) analysis. The cells were grown in DMEM (low glucose) (Sigma-Aldrich; Merck KGaA) at 37˚C with 5% CO_2. pcDNA3-Flag-IDH1-R132H was a kind gift from Dr Yue Xiong (Addgene plasmid cat. no. 62907; http://n2t.net/addgene:62907; RRID: Addgene_62907; Addgene, Inc.) (10). Pure colonies were selected from ampicillin-containing LB agar plates and then grown in LB broth (MilliporeSigma) at 37˚C. Plasmid DNA was then isolated using the SmartPure Plasmid DNA Isolation kit (Eurogentech). The DNA (10 μg/ml) mixed with transfection reagent and its buffer was used for transfecting the glioma cells ($1x10^4$ cells) cultured in a 12-well culture plate. Transfection was performed using the Jetprime transfection kit (Polyplus-transfection SA) for 4 h in serum-free DMEM and the medium was changed to 10% FBS-containing medium after 4 h. The cells were used for the experiments after 48 h. The concentrations of 2-HG, N-acetylcysteine (NAC) and mutant IDH1 inhibitor used were reported earlier in various studies (11,12). A total of 30 mM 2-HG, 2 μM mIDH1 inhibitor (AGI-5198) and 1 mM NAC (all from Sigma-Aldrich; Merck KGaA) were used for the experiments.

Intracellular ROS measurements. The intracellular ROS levels were measured in cultured cells after the various treatments using dichlorodihydrofluorescein diacetate (DCF-DA; D6883-50MG; Sigma-Aldrich; Merck KGaA). The cells were cultured in a 96-well black plate at a seeding density of $1x10^4$ cells per well. The wells were washed with HBSS (MilliporeSigma) after treatment and incubated with 10 μM DCFH-DA at 37˚C in the dark for 1 h. The cells treated with 100 μM H_2O_2 (MilliporeSigma) for 30 min were used as a positive control. The wells were washed twice with HBSS to remove excess dye, and the DCF fluorescence developed was measured using a fluorimeter (BioTek instruments, Inc.) at 530 nm (excitation 488 nm), using Gen5 softwarev2.0 (BioTek instruments, Inc.). The relative fluorescence of the treated groups to the control was calculated using the fluorescence intensities from triplicates.

Western blot analysis. The cells and glioma tissues were processed for protein expression analysis and probed for desired proteins along with loading controls. The culture plates having either U87MG or U251MG cells were decanted off the medium and washed thrice thoroughly with ice-cold PBS to remove all traces of media and other chemicals. After decanting off the PBS, the cells were incubated for 5 min in ice-cold radio immunoprecipitation assay (RIPA) (Thermo Fisher Scientific, Inc.) buffer containing protease/phosphatase inhibitor cocktail. The cells were scraped using a cell scraper and the lysate was then collected in a microcentrifuge tube. The lysates were then incubated 30 min in ice with vortexing at regular intervals of 5 min. The cell lysates were centrifuged at 16,500 x g for 15 min at 4˚C and the supernatants were stored at -80˚C. The glioma and as non-tumor tissues after weighing were pulverized using RIPA buffer with protease/phosphatase inhibitor cocktail (Thermo Fisher Scientific, Inc.). The supernatant was collected and stored as mentioned above. The isolated proteins were quantified using the bicinchoninic acid assay method (Pierce; Thermo Fisher Scientific, Inc.).

The protein lysates (30-60 μg) were mixed with 6X Laemmli buffer containing 2-mercaptoethanol (2-ME) (Thermo Fisher Scientific, Inc.), heat denatured for 5 min at 95˚C and resolved on 5-12% polyacrylamide gels using Tris-Glycine-SDS buffer. The resolved proteins were transferred to a PVDF membrane (pre-wetted with 100% methanol) using a Trans semi-dry blot apparatus (Bio-Rad Laboratories, Inc.) at 10 V for 30-40 min. The membrane was blocked for 1 h at room temperature using either 5% skimmed milk (for non-phosphoprotein detection) or 1% bovine serum albumin (BSA) solutions in TBST. The membrane was then probed with antibodies (prepared in 3% BSA-TBST) specific to the target proteins at 4˚C overnight. Secondary antibodies conjugated to horseradish peroxidase (HRP; anti-rabbit IgG; cat. no. 7074S; 1:5,000-1:8,000; anti-mouse IgG; cat. no. 7076; 1:10,000-1:20,000; both secondary antibodies were from Cell Signaling Technology, Inc.) were used to probe the primary antibodies by incubation for 1 h at room temperature. Protein bands were visualized using Enhanced Chemiluminescence

Table I. Summary of the patient characteristics.

No. of cases	Tumor grade	Age (range)	Sex	
			Female	Male
17	LGG	11-65	8	9
40	HGG	7-63	11	29

(Thermo Fisher Scientific, Inc.) detection. Equal volumes of luminol and peroxide solutions were mixed and added on to the membranes. Light emitting bands were captured on an X-ray film and developed and then documented in Gel Doc™ XR Imaging System (Bio-Rad Laboratories, Inc.) and quantified using Quantity One 1 D Analysis Software (Version 4.6.7, Bio-Rad Laboratories, Inc.).

The primary antibodies used were as follows: MTH1 (1:500; cat. no. NB100-109, Novus Biologicals, Inc.), vinculin (;1:1,000; cat. no. 13901, Cell Signaling Technology, Inc.), manganese superoxide dismutase (Mn-SOD; 1:1,000; cat. no. ab68155, Abcam), glutathione peroxidase (GPx; 1;1,000; cat. no. ab125066, Abcam), mIDH1 (1:500; cat. no. SAB4200548), FLAG (1:500; cat. no. F2555) and β-actin (1:2,000; cat. no. A2228) (all from Sigma-Aldrich; Merck KGaA).

Enzyme immunoassays. The Universal 8-oxo-dG ELISA kit (ImmunoTag) was used in order to measure the levels of 8-oxo-dG, which is an indicator of MTH1 activity. The cells/tissue lysates were prepared according to the protocol provided with the kit and added in triplicate into the 96-well plate coated with antibody against 8-oxo-dG. Briefly, the biotinylated antibodies were added which was followed by streptavidin-HRP for labeling. The substrate (provided with the kit) for HRP was then added for color development and the reaction was terminated after 10 min. The absorbance was then measured at 450 nm using an ELISA plate reader (BioTek Instruments, Inc.) and the 8-oxo-dG concentrations were extrapolated from their respective standard curves.

Immunofluorescence staining. 8-Oxoguanineglycosylase-1 (OGG1) expression was analyzed in the cells using immunocytochemistry. Briefly, the cells were fixed, permeabilized and incubated with blocking buffer. The cells were then incubated with anti-OGG1 antibody (1:200; (cat. no. ITA6482; ImmunoTag) for overnight at 4˚C. After washing, the cells incubated with secondary antibody (anti-rabbit; 1:10,000; Cell Signaling Technology, Inc.; cat. no. 7074S) and then observed under a fluorescence microscope (Olympus Corporation) once stained with DAPI (Sigma-Aldrich; Merck KGaA) for 15 min in the dark at room temperature. The images captured were analyzed using ImageJ software v1.49 (National Institutes of Health) and the mean fluorescence intensity normalized to the cell count was estimated.

Sanger sequencing. Genomic DNA from frozen tissue sections from the glioma tissue biopsies was isolated using the HiPura™ Mammalian Genomic DNA Purification kit (HiMedia). The target region (Exon 4 of IDH1) was amplified using the following forward and reverse primer set: IDH1 forward, 5'-CGGTCTTCAGAGAAGCCATT-3' and reverse, 5'-GCAAAATCACATTATTGCCAAC-3'. A total of 50 ng isolated DNA was amplified using the primers for 30 cycles (95˚C for 40 sec, 60˚C for 40 sec, and 72˚C for 1 min). following the purification of the PCR product, cycle sequencing was carried out using the ABI Big Dye Terminator v.3.1 kit (Thermo Fisher Scientific, Inc.). PCR products were resolved by electrophoresis on an 8 capillary ABI 3500 model sequencer (Thermo Fisher Scientific, Inc.). In this case, cycle sequencing was performed separately in both the forward and reverse directions. The sequences obtained were analyzed using the BioEdit tool (Tom Hall, Ibis Biosciences) and the corresponding genotypes were recorded.

Statistical analysis. All data are presented as the mean ± SEM. Statistical analyses were performed using GraphPad Prism 5 software (GraphPad Software, Inc.). The Shapiro-Wilk test was used to test the normality of the data. Non-parametric tests were used for those data which were not normally distributed. Parametric tests were used for those data which were normally distributed. For comparisons between two groups, an unpaired t-test was used for cell line data and the Mann Whitney test for patient-derived data. In case of multiple group comparisons, for parametric analysis, one-way ANOVA followed by Tukey's or Dunnett's multiple comparisons test was performed. For non-parametric analysis, the Kruskal-Wallis test with Dunn's post hoc test were used. Pearson's correlation coefficient was used for examining the correlation between MTH1 and mIDH1 expression. P-values ≤0.05 were considered to indicate statistically significant differences.

Results

mIDH1 expression and 2-HG-treatment enhance the MTH1 levels in glioma cells. In order to examine whether mIDH1 has any effect on the expression of MTH1, a FLAG-tagged plasmid carrying the mutant IDH1 (R132H) was expressed in the U87MG and U251MG cells. FLAG expression indicating successful transfection is illustrated in (Fig. 1A). Western blot analysis of the protein isolated from U87MG cells revealed that MTH1 expression was significantly increased (P<0.0001, 2.79±1.22; Fig. 1B) in mIDH1-expressing cells compared to the empty vector-transfected wt-IDH1 cells. Upon the inhibition of mIDH1 using a specific inhibitor (AGI-5198), the MTH1 protein levels were significantly decreased P<0.0001, 1.37±0.07; (Fig. 1B). Similar results were also obtained with the U251 cells (Fig. 1C). Subsequently, the U87MG cells treated with 2-HG exhibited a significant increase in MTH1 expression (P=0.0308, 1.65±0.20) compared to the untreated control (Fig. 1D). When examining the expression of OGG1, a base excision repair enzyme, its expression was significantly increased in mIDH1-expressing and 2-HG-treated U251 cells; however, upon the inhibition of mIDH1 with its specific inhibitor, its expression was reduced (Fig. 1E).

mIDH1/2-HG contributes to high ROS levels in glioma cells. The DCF-DA assay was performed to determine whether ROS are produced due to mIDH1 expression or its product, 2-HG,

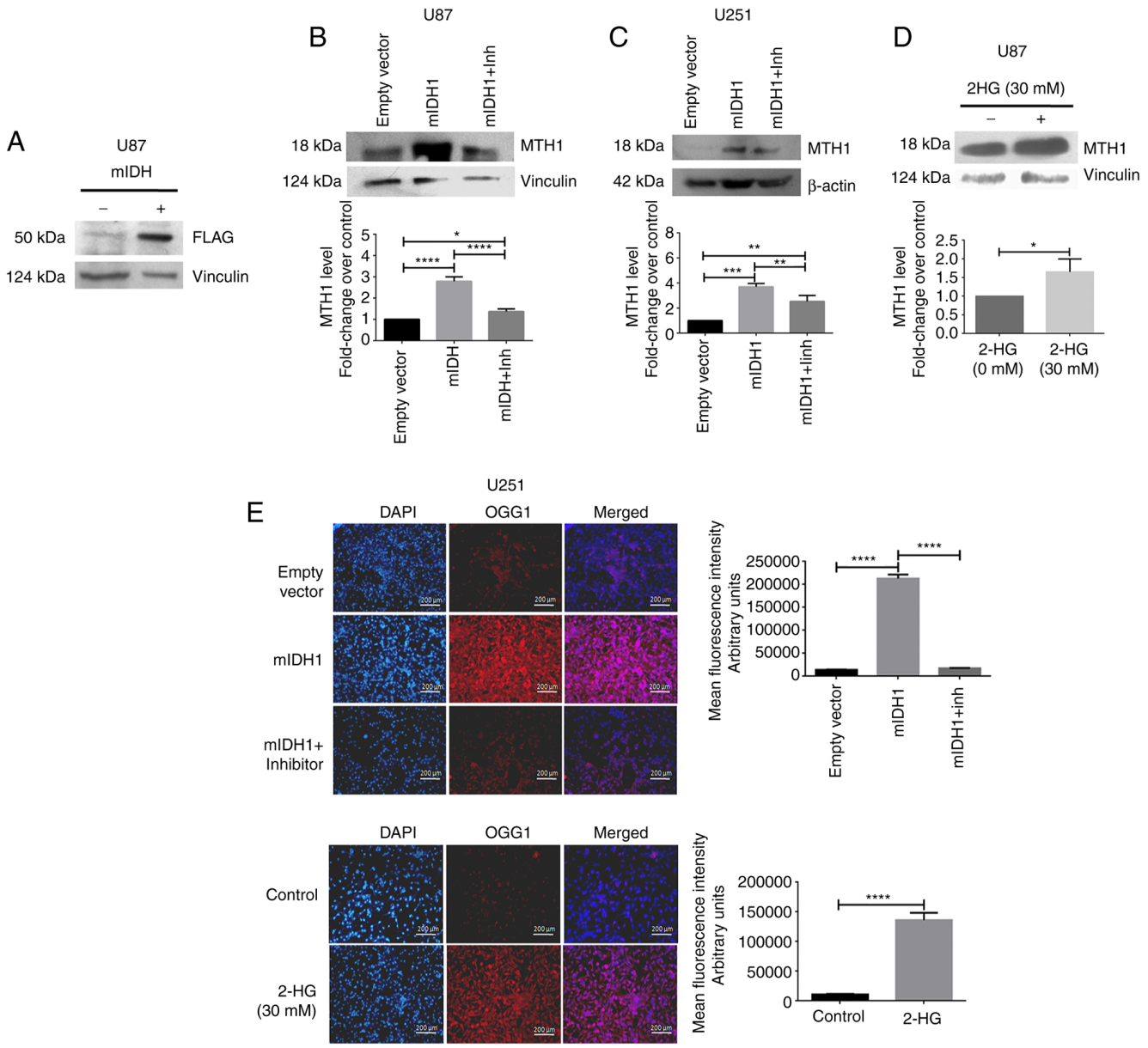

Figure 1. mIDH1 expression and 2-HG-treatment enhances MTH1 levels in glioma cells. (A) Western blots representing the FLAG expression, illustrating the *mIDH1* transfection efficiency in U87 cells. (B) Western blot analysis showing the expression of MTH1 in mIDH1 expressing and mIDH1 inhibited U87 cells. The mIDH1 inhibitor, AGI-5198, was used at a concentration of 2 μM for 24 h. Vinculin was used as the internal control. Statistical analysis was performed using ANOVA with Tukey's multiple comparison tests. *P<0.05 and ****P<0.0001 (n=4). (C) Western blot analysis of MTH1 expression in mIDH1-expressing cells and in U251 cells in which mIDH1 was inhibited. β-actin was used as the loading control. **P<0.01 and ***P<0.001 (n=3). (D) Western blot analysis of the expression of MTH1 in 2-HG-treated U87 cells. Vinculin was used as the internal control. Statistical analysis was performed using a Student's t-test. *P<0.05 (n=3). (E) Representative images of immunofluorescence staining of OGG1 expression in mIDH1-expressing and 2-HG-treated U251 cells; Statistical analysis was performed using ANOVA with Tukey's multiple comparison tests; ****P<0.0001 (n=3). mIDH1, mutant isocitrate dehydrogenase 1; 2-HG, 2-hydroxyglutarate; MTH1, MutT homolog 1.

in U87 cells. Cells transfected with plasmid carrying mIDH1 or treated with 2-HG were subjected to fluorometric analysis for the detection of ROS. The measurements of DCF fluorescence revealed a significant increase in the ROS levels in cells expressing mIDH1. The mIDH1-expressing cells exhibited a 8.51-fold increase in fluorescence intensity (P<0.0001, 422.7±7.45) than cells harboring the empty vector (49.67±1.67) (Fig. 2A). In addition, in the 2-HG-treated cells, the ROS fluorescence levels were increased 7.0-fold (P<0.0001, 443±13.43) when compared to the untreated control (63.33±3.18). (Fig. 2B). Moreover, in mIDH1-expressing cells treated with the specific mIDH1 inhibitor, DCF fluorescence decreased 3.4-fold (P<0.0001, 112±7.94) vs. the mIDH1-expressing cells (Fig. 2A).

Pre-treatment of both mIDH1-expressing cells and 2-HG-treated cells with NAC, a ROS scavenger, prevented the inhibition of the formation of ROS under these conditions (6.06-fold, P<0.0001, 384±19.92; and 7.67-fold, P<0.0001, 381±16.56, respectively) compared to the respective control groups (Fig. 2A and B). H_2O_2 was used as a positive control in these experiments. In addition, the levels of the two antioxidant enzymes, GPx4 and MnSOD, were determined upon treatment of the U87MG cells with 2-HG using western blot analysis. The levels of the antioxidant enzymes, GPx4

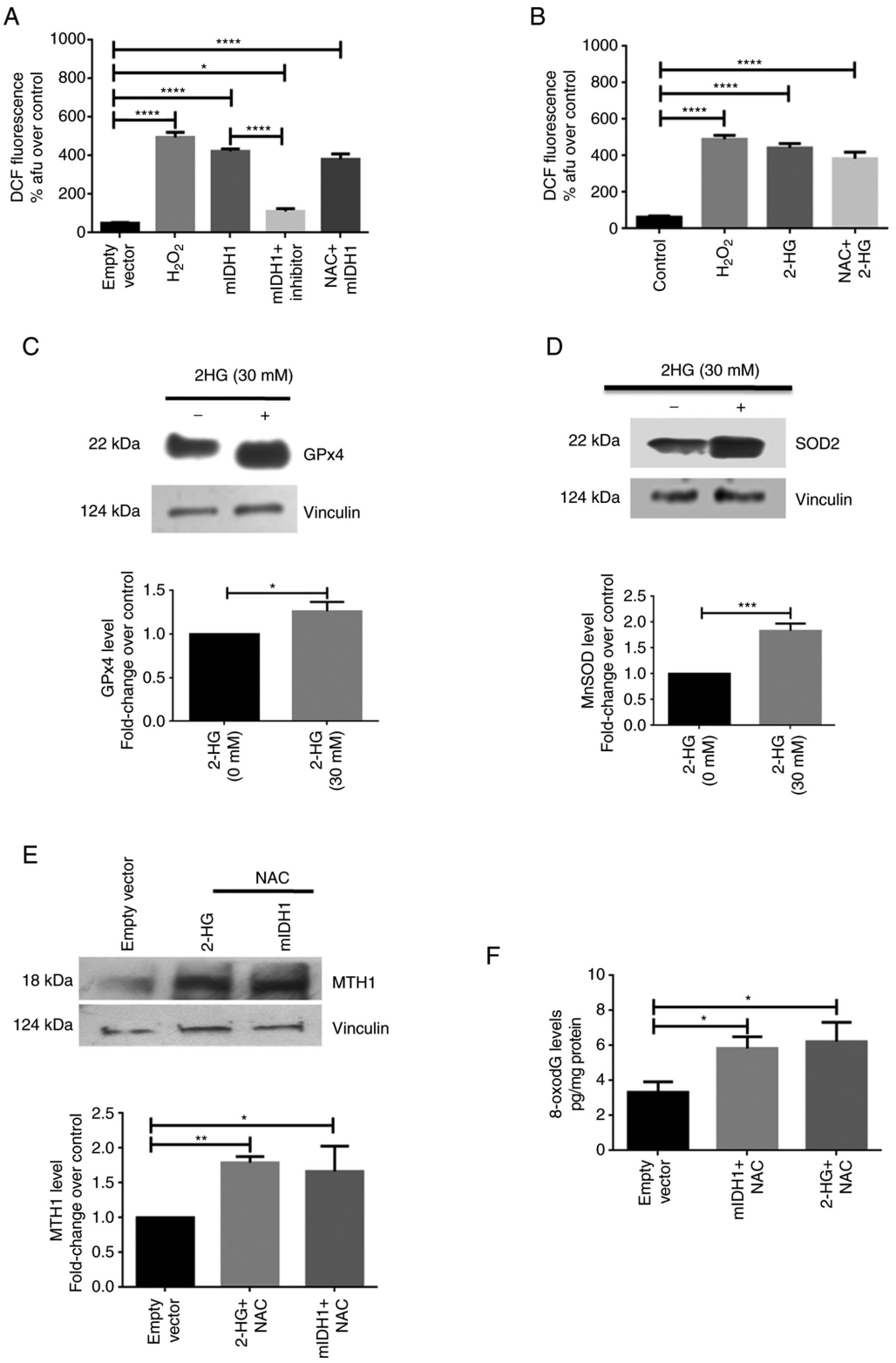

Figure 2. mIDH1/2-HG contributes to high ROS levels in glioma cells. (A) Histograms representing ROS levels measured by DCFHDA fluorimetric analysis on U87 cells transfected with the mIDH1-R132H plasmid. Statistical analysis was performed using ANOVA with Tukey's multiple comparison tests. *P<0.05 and ****P<0.0001 (n=3). (B) Histograms representing ROS levels measured by DCFHDA fluorimetric analysis on treating U87 cells treated with 30 mM 2-HG for 48 h. Statistical analysis was performed using ANOVA with Tukey's multiple comparison tests. ****P<0.0001 (n=3). (C) Representative western blots and histogram illustrating increased the expression of GPx4 in U87 cells treated with 30 mM 2-HG for 48 h. Vinculin was used as the internal control. Statistical analysis was performed using the Student's t-test. *P<0.05 (n=3). (D) Western blot analysis demonstrating the increased expression of MnSOD in U87 cells treated with 30 mM 2-HG. Vinculin was used as the internal control (the same internal control as shown in Fig. 1D as the blots are from the same gel). Statistical analysis was performed using the Student's t-test. ***P<0.001 (n=3). (E) Representative western blots illustrating MTH1 expression in U87 cells pre-treated with 1 mM NAC, a ROS scavenger and subsequently either transfected with mIDH1 or treated with 30 mM 2-HG for 48 h. Vinculin was used as the internal control. Statistical analysis was performed using ANOVA with Tukey's multiple comparison tests. *P<0.05 and **P<0.01 (n=3). (F) Histogram representation of 8-oxodG levels in U87 cells with the above treatments. Statistical analysis was performed using ANOVA with Tukey's multiple comparison tests. *P<0.05 (n=3). mIDH1, mutant isocitrate dehydrogenase 1; 2-HG, 2-hydroxyglutarate; MTH1, MutT homolog 1; NAC, N-acetylcysteine; 8-oxodG, 8-oxo-7,8-dihydro-2'-deoxyguanosine; afu, arbitrary fluorescence unit.

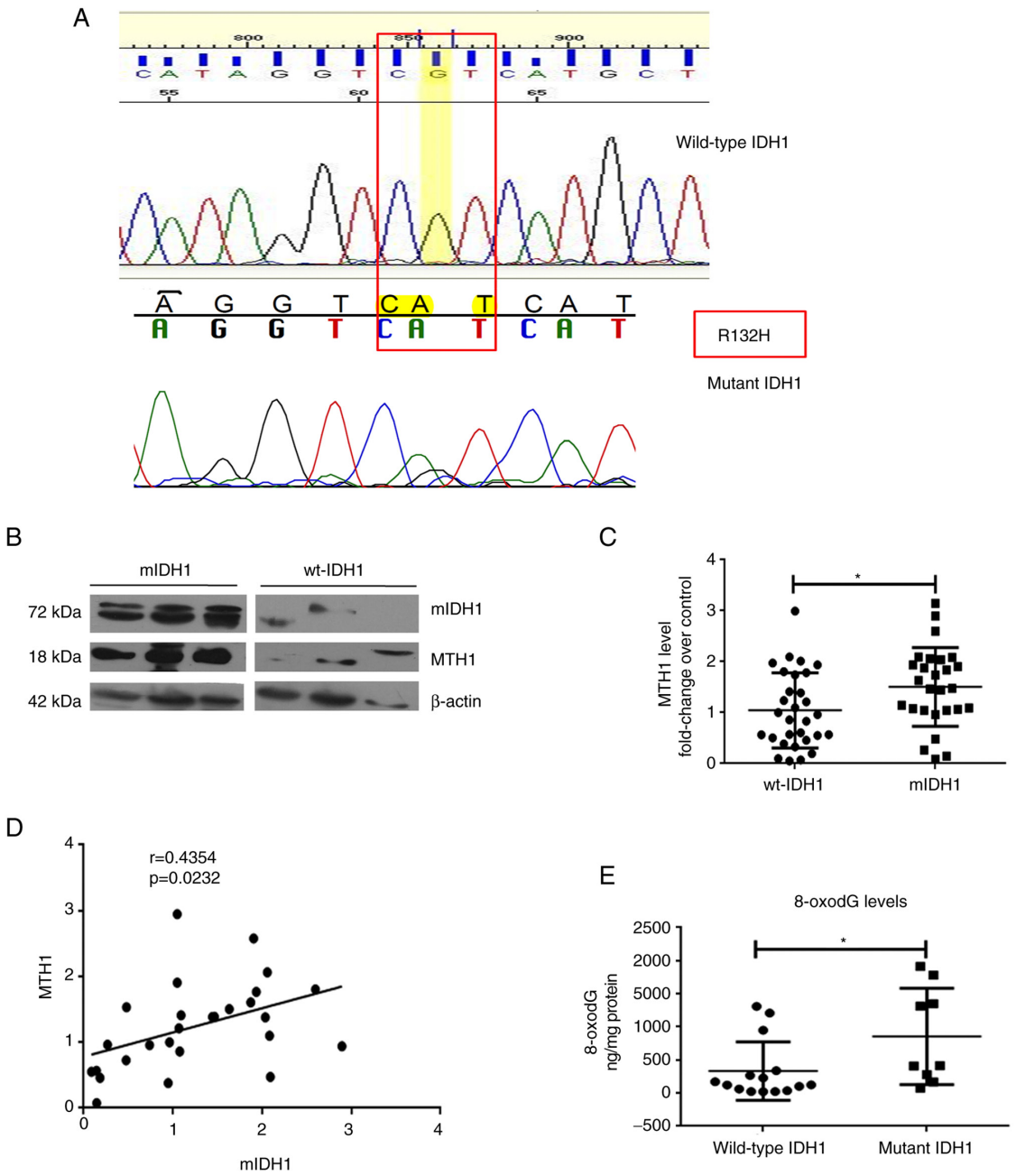

Figure 3. Glioma tissues harboring mIDH1 exhibit an increased MTH1 expression and activity. (A) Sequencing data illustrating the IDH1 R132H mutation in samples from patients with glioma (n=21). (B) Representative western blots demonstrating MTH1 expression in glioma tissues (wt-IDH1, n=30; mIDH1, n=27). β-actin was used as the internal control. (C) Dot plot representation of MTH1 expression in glioma tissues with and without IDH1 mutation. Statistical analysis was performed using the Mann-Whitney test. *P<0.05. (D) Scatter plot demonstrating the correlation of MTH1 with mIDH1 in samples from patients with glioma (r=0.4354, P=0.0232). Pearson's correlation analysis was used (n=27). (E) Dot plot representation of 8-oxodG levels in samples from patients with glioma with mIDH1 compared with samples without IDH1 mutation. Statistical analysis was performed using the Mann-Whitney test. *P<0.05. mIDH1, mutant isocitrate dehydrogenase 1; MTH1, MutT homolog 1.

(P=0.0136, 1.26±0.06) and MnSOD (P=0.0005, 1.83±0.08), were increased in the presence of 2-HG (Fig. 2C and D).

The U87 MG cells expressing mIDH1 were pre-treated with 1 mM NAC for 24 h and then probed for MTH1 protein levels. In another group, NAC-pre-treated U87MG cells were exposed to 30 mM 2-HG for 48 h. Western blot analysis of proteins isolated from these NAC-pre-treated cells exhibited an elevated MTH1 expression both following mIDH1 transfection (P=0.0158, 1.67±0.21) and 2-HG treatment (P=0.0073, 1.79±0.05) (Fig. 2E). A significant increase in 8-oxodG levels was also observed in the NAC-pre-treated cells expressing mIDH1 (P=0.0218, 5.84±0.38), as well as in those treated with 2-HG (P=0.0115, 6.23±0.63) (Fig. 2F).

Increased MTH1 expression and activity in mIDH1-harboring glioma tissues. The DNA sequencing data of a subset of patient samples (n=21) denoting the IDH1 status revealed that 5 patients had the R132H mutation (Fig. 3A). Out of the 57 glioma samples, MTH1 expression was found to be elevated in patients harboring mIDH1 when compared to those harboring wt-IDH1. Western blot analyses of the glioma tissues revealed that MTH1 expression was significantly upregulated

(P=0.0249) in patients harboring the mIDH1 (n=27, 1.51±0.15) when compared to patients carrying wt-IDH1 (n=30, 1.04±0.13) (Fig. 3B and C). In patients with mIDH1, there was a moderate positive correlation between mIDH1 and MTH1 expression (n=27; r=0.4354, P=0.0232) (Fig. 3D).

Subsequently, the 8-oxo-dG levels, which are indicative of the activity of the MTH1 enzyme, were measured in glioma tissue biopsy extracts using immunoassay. The results revealed increased 8-oxo-dG levels in those patients harboring mIDH1 (n=15; 855.3±242.6 ng/mg) compared to patients with wt-IDH1 (n=9; 332.6±114.1 ng/mg; P=0.0148; Fig. 3E), which was in concordance with the correlation found between MTH1 and mIDH1 expression. This indicated that concurrent with the high MTH1 expression pattern observed in the mIDH1 glioma samples, there was a relative increase in MTH1 activity as well.

Discussion

The oxidative damage of biomolecules, such as proteins, DNA and lipids due to elevated ROS levels promotes pro-tumorigenic signaling, cancer cell proliferation, cell survival, cancer metastasis, apoptosis, and adaptation to hypoxia (13,14). Research pertaining to IDH mutations in the pathobiology of cancers, particularly gliomas is increasing worldwide. The R132H substitution, the frequently observed IDH1 mutation in gliomas is caused by the G→A transition at nucleotide position 395 of codon 132 (15). Cancer-associated IDH mutations lead to the formation of an oncometabolite, 2-HG (16) and an associated increased ROS environment in cells and subsequent oxidative stress, which is a major hallmark of cancers with IDH mutations (17). 2-HG, being the structural analogue of α-KG, competitively inhibits various α-KG-dependent enzymes, α-keto acid transaminase, the inhibition of DNA break repair and the methylation of histones, such as H3K4, H3K9 and H3K27 (15-18).

Since increased ROS levels are associated with a greater propensity for oxidant-mediated DNA damage in cells, it was hypothesized that mIDH1/2-HG may induce the expression of MTH1, an enzyme responsible for sanitizing the oxidant nucleotide pool in cells. The results of the present study are in line with the initial hypothesis of the authors (as aforementioned), and 2-HG-treated and mIDH1-expressing U87MG, as well as U251 cells, exhibited a high level of MTH1 expression. The increased MTH1 expression in mIDH1-expressing cells was significantly decreased upon treatment with a specific mIDH1 inhibitor (AGI-5198), which establishes the role of mIDH1/2-HG in regulating MTH1 levels in cells.

Augmented ROS levels observed in both mIDH1-expressing and 2-HG-treated cells are in concordance with an earlier report (11). This shift in the redox status of cells is likely to trigger the escalation of the antioxidant enzymes, GPx4 and MnSOD, as was observed herein. In order to examine whether the obliteration of basal ROS would significantly affect the pro-oxidant influences imparted by mIDH1/2-HG, the cells were pre-treated with NAC and probed for ROS levels. Notably, NAC pre-treatment had little or no influence on the ROS-inducing capabilities of mIDH1/2-HG. When probed for MTH1 expression under NAC pre-treatment in mIDH1/2-HG treated cells, there was almost a 2-fold increase in protein levels and in MTH1 enzyme activity, determined by the 8-oxodG levels in cells. These results indicate the augmented MTH1 activity in the treated cells, even after scavenging the basal ROS that clearly suggests ROS generated via mIDH1/2-HG are responsible for the activation MTH1 in glioma cells.

Of note, in glioma patient biopsies with IDH1 mutation, a significantly higher MTH1 expression was observed compared to the wt-IDH1 samples. A concomitant increase in the activity (as assessed by the increased 8-oxo-dG levels) supported the protein expression results in glioma tissues.

The highlight of the present study is that a link was found between mIDH1 and MTH1 activation, mediated by ROS. This forms the basis for the increased MTH1 expression observed in mIDH1 glioma tissues and is the first study (to the best of our knowledge) linking IDH1 mutation, ROS and activation of MTH1 in cells. As it was found that mIDH1/2-HG causes increased DNA damage (a higher OGG1 expression) in U251 cells, this may yet be another factor that plays a role in the upregulation of MTH1 in gliomas. Further experiments are required in order to decipher the mechanistic molecules involved in relation to MTH1 and mIDH1.

Acknowledgements

The authors would like to acknowledge Dr Priya Srinivas (Scientist-G, Rajiv Gandhi Centre for Biotechnology, Kerala, India) and Dr Cibin Raghavan (Associate Professor, Sree Chitra Tirunal Institute for Medical Sciences and Technology, Kerala, India) for their valuable inputs and suggestions towards execution of the study. The authors would also like to thank Dr Jackson James (Scientist-G, Rajiv Gandhi Centre for Biotechnology, Kerala, India) for providing the empty vector for the mIDH1 overexpression studies.

Funding

The authors would like to thank the Department of Science and Technology, India for providing the INSPIRE Fellowship (IF150784). The authors also acknowledge the Council of Scientific and Industrial Research [09/523(0082)/2014-EMR-1], Government of India for granting Research Fellowship.

Availability of data and materials

The datasets generated during and/or analyzed during the current study are available from the corresponding author on reasonable request.

Authors' contributions

BB, CRA, MU, KS, AND and SG were involved in the conceptualization and methodology of the study. BB, CRA, MU, HVE, KS, GRM, KK, AND and SG were involved in data validation. BB, CRA, MU, HVE, KS, GRE, KK, AND and SG were involved in the formal analysis. BB, CRA, HVE, KS, GRE and KK were involved in the provision of the study resources. BB, CRA, MU and SG were involved in the writing of the original draft and visualization. BB, CRA, MU and SG were involved in the writing, reviewing and editing of the manuscript. MU and SG supervised the study. SG was

involved in project administration and in funding acquisition. All authors have read and approved the final manuscript. BB and CRA confirm the authenticity of the raw data. All authors have read and approved the final manuscript.

Ethics approval and consent to participate

All procedures performed with human subjects in the present study were in accordance with the ethical standards of the Institutional Ethics Committee of Sree Chitra Tirunal Institute for Medical Sciences and Technology, Trivandrum, India, and with the 1964 Helsinki declaration and its later amendments or comparable standards. Informed consent was obtained from all individual participants >18 years of age included in the study. Informed consent was obtained from the parents of the patients who were <18 years of age included in the study.

Patient consent for publication

Not applicable.

Competing interests

The authors declare that they have no competing interests.

References

1. Han S, Liu Y, Cai SJ, Qian M, Ding J, Larion M, Gilbert MR and Yang C: IDH mutation in glioma: Molecular mechanisms and potential therapeutic targets. Br J Cancer 122: 1580-1589, 2020.
2. Shi J, Zuo H, Ni L, Xia L, Zhao L, Gong M, Nie D, Gong P, Cui D, Shi W and Chen J: An IDH1 mutation inhibits growth of glioma cells via GSH depletion and ROS generation. Neurol Sci 35: 839-845, 2014.
3. Parsons DW, Jones S, Zhang X, Lin JC, Leary RJ, Angenendt P, Mankoo P, Carter H, Siu IM, Gallia GL, *et al*: An integrated genomic analysis of human glioblastoma multiforme. Science 321: 1807-1812, 2008.
4. Komori T: The 2021 WHO classification of tumors, 5th edition, central nervous system tumors: The 10 basic principles. Brain Tumor Pathol 39: 47-50, 2022.
5. Louis DN, Perry A, Reifenberger G, von Deimling A, Figarella-Branger D, Cavenee WK, Ohgaki H, Wiestler OD, Kleihues P and Ellison DW: The 2016 World Health Organization classification of tumors of the central nervous system: A summary. Acta Neuropathol 131: 803-820, 2016.
6. Molenaar RJ, Botman D, Smits MA, Hira VV, van Lith SA, Stap J, Henneman P, Khurshed M, Lenting K, Mul AN, *et al*: Radioprotection of IDH1-mutated cancer cells by the IDH1-mutant inhibitor AGI-5198. Cancer Res 75: 4790-4802, 2015.
7. Qing X, Shao Z, Lv X, Pu F, Gao F, Liu L and Shi D: Anticancer effect of (S)-crizotinib on osteosarcoma cells by targeting MTH1 and activating reactive oxygen species. Anticancer Drugs 29: 341-352, 2018.
8. Gad H, Koolmeister T, Jemth AS, Eshtad S, Jacques SA, Ström CE, Svensson LM, Schultz N, Lundbäck T, Einarsdottir BO, *et al*: MTH1 inhibition eradicates cancer by preventing sanitation of the dNTP pool. Nature 508: 215-221, 2014.
9. Bhavya B, Easwer HV, Vilanilam GC, Anand CR, Sreelakshmi K, Urulangodi M, Rajalakshmi P, Neena I, Padmakrishnan CJ, Menon GR, *et al*: MutT homolog1 has multifaceted role in glioma and is under the apparent orchestration by hypoxia inducible factor1 alpha. Life Sci 264: 118673, 2020.
10. Zhao S, Lin Y, Xu W, Jiang W, Zha Z, Wang P, Yu W, Li Z, Gong L, Peng Y, *et al*: Glioma-derived mutations in IDH1 dominantly inhibit IDH1 catalytic activity and induce HIF-1alpha. Science 324: 261-265, 2009.
11. Gilbert MR, Liu Y, Neltner J, Pu H, Morris A, Sunkara M, Pittman T, Kyprianou N and Horbinski C: Autophagy and oxidative stress in gliomas with IDH1 mutations. Acta Neuropathol 127: 221-233, 2014.
12. Chen L, Li X, Liu L, Yu B, Xue Y and Liu Y: Erastin sensitizes glioblastoma cells to temozolomide by restraining xCT and cystathionine-γ-lyase function. Oncol Rep 33: 1465-1474, 2015.
13. Behrend L, Henderson G and Zwacka RM: Reactive oxygen species in oncogenic transformation. Biochem Soc Trans 31: 1441-1444, 2003.
14. Reczek CR and Chandel NS: The two faces of reactive oxygen species in cancer. Annu Rev Cancer Biol 1: 79-98, 2017.
15. Mohamed Yusoff AA, Zulfakhar FN, Sul'ain MD, Idris Z and Abdullah JM: Association of the IDH1 C.395G>A (R132H) mutation with histological type in malay brain tumors. Asian Pac J Cancer Prev 17: 5195-5201, 2016.
16. Bhavya B, Anand CR, Madhusoodanan UK, Rajalakshmi P, Krishnakumar K, Easwer HV, Deepti AN and Gopala S: To be wild or mutant: Role of isocitrate dehydrogenase 1 (IDH1) and 2-hydroxy glutarate (2-HG) in gliomagenesis and treatment outcome in glioma. Cell Mol Neurobiol 40: 53-63, 2020.
17. Shi J, Sun B, Shi W, Zuo H, Cui D, Ni L and Chen J: Decreasing GSH and increasing ROS in chemosensitivity gliomas with IDH1 mutation. Tumour Biol 36: 655-662, 2015.
18. Reiter-Brennan C, Semmler L and Klein A: The effects of 2-hydroxyglutarate on the tumorigenesis of gliomas. Contemp Oncol (Pozn) 22: 215-222, 2018.